

RESEARCH ARTICLE

Cognitive information delivery in geo-location database based cognitive radio networks

Zhiyong Feng^{1*}, Zhiqing Wei¹, Qixun Zhang¹, Wei Li², Xin Wang³ and Yi Qian⁴¹ Beijing University of Posts and Telecommunications, China² University of Victoria, Canada³ Stony Brook University, USA⁴ University of Nebraska–Lincoln, USA

ABSTRACT

For the problem of spectrum scarcity and wastage, cognitive radio (CR) technology provides a solution to utilizing the vacant spectrum more efficiently. As one of the most promising techniques to obtain the cognitive information in TV white spaces, geo-location database approach has attracted a lot of recent attentions, with its goal of enhancing the efficiency of spectrum usage and avoiding the interference to TV receivers. However, existing works mainly focus on the construction and applications of geo-location database, and seldom consider how to deliver the cognitive information from the database to TV band devices. In this paper, we investigate the tradeoff between increasing the accuracy of cognitive information delivery and reducing the overhead. We design two mesh fusion algorithms to reduce the redundancy of cognitive information and improve the efficiency of cognitive information delivery. Finally, we verify our analysis and evaluate the efficiency of the proposed mesh fusion algorithms through numerical studies. Copyright © 2016 John Wiley & Sons, Ltd.

KEYWORDS

cognitive radio networks; TV white spaces; cognitive information; mesh fusion algorithm

*Correspondence

Zhiyong Feng, Xitucheng Road, Haidian District, Beijing 100876, China.

E-mail: fengzy@bupt.edu.cn

1. INTRODUCTION

Wireless networks are facing a big challenge because of the explosively growing data service demands. According to the reports in [1], the monthly global mobile data traffic is expected to surpass 10 exabytes by 2016. This skyrocketing spectrum demand cannot be met by traditional spectrum allocation strategy, where fixed and fragmented spectrum bands lead to spectrum scarcity. On the other hand, most of the spectrum bands are under-utilized [2], which result in the spectrum wastage. This includes the TV white spaces (TVWSs), which are the available spectrum bands of TV networks in the dimensions of space, time and spectrum, and others. To address the problems of spectrum scarcity and wastage, cognitive radio (CR) technology has attracted many recent research interests. A CR device has the abilities to be aware of its environment, dynamically and autonomously adjust its operational parameters and protocols, and learn from the experiences, in order to improve the efficiency of spectrum utilization.

As the crucial components for CR enabling, three technologies have been considered to obtain the knowledge of

the operational radios and the geographical environments in cognitive radio systems: spectrum sensing [3], beaconing [4] (which includes cognitive pilot channel (CPC) and common control channel (CCC)), and geo-location database. Consensus on the use of the three techniques has been reached in the International Telecommunication Union [5]. Furthermore, both Federal Communications Commission and European Conference of Postal and Telecommunications Administrations have released rules, orders, and technical specifications to allow unlicensed radio transmitters or TV band devices (TVBDs) to operate at the TVWS based on the geo-location database approach [6–8]. Note that spectrum sensing faces the challenge of addressing the hidden node problem. Beaconing and CPC need a permanent channel. Compared with them, the geo-location database approach is regarded as one of the promising solutions for gaining accurate and efficient environment awareness to enhance the spectrum usage and avoid the interference to the licensed TV receivers.

The geo-location database is defined as a digital archive that acquires, processes, stores, and delivers the available spectrum band information in [9]. The geo-location

database approach can be applied to control the interference to TV receivers [10], to exploit both spatial and spectral degrees-of-freedom by using low-powered devices [11], to support the smart utility network[†] application scenarios in TVWS [12], and to support the broadband through TVWS and a wireless conferencing system [9].

Although there are many studies on the geo-location database approach, existing studies mainly focus on the construction and applications of geo-location database. CR nodes need to access geo-location database to obtain spectrum information to guide their transmissions. However, there is little work on how to efficiently deliver the cognitive information from the database to TVBDs and to understand the key factors that affect the performance of CR systems. It is unclear when the geo-location database needs to be accessed and how often to access the database. These could have significant impact on the CR performance, the load of accessing geo-location database, and the overall possibility of applying the database method to support CR operations.

With the support of geo-location database in TVWSs, a TVBD obtains the local channel occupancy information by sending its location to the database. The information on the channels locally available is defined as *cognitive information* in this paper. When a TVBD is mobile, it is difficult to determine when to access the database. If the TVBD queries the database at a small moving distance, it will cost more energy of TVBD and increase the accessing load of the database. On the contrary, if the TVBD requests cognitive information when it moves a long distance, the error of cognitive information will be very large. If the cognitive information delivery is not accurate enough, vacant spectrum resources will not be efficiently utilized, and the interference to TV receivers will increase. Therefore, the accuracy and efficiency of the cognitive information delivery from geo-location database to TVBD will affect the efficiency of spectrum usage and the interference to TV receivers.

In this paper, we first analyze the tradeoff between the accuracy and efficiency of cognitive information delivery. We further design mesh fusion algorithms (MFAs) to fuse the adjacent meshes with the same cognitive information to reduce the redundancy and improve the efficiency of cognitive information delivery without compromising the accuracy. Notice that this paper refers to some conclusions in our conference papers [13][14]; however, the theme of this paper is different from our conference papers, and we have improved our previous work in this paper, including cognitive information delivery problem proposed in this paper, rewriting the proof of Theorem 2, the new Theorem 3, the algorithm analysis, and more detailed simulations.

The rest of this paper is organized as follows. We present the related work in Section 2. The problem statement is presented in Section 3. The tradeoffs between the size of mesh and the accuracy of cognitive information are stud-

ied in Section 4. In Section 5, the MFAs are designed to improve the efficiency of cognitive information delivery. In Section 6, numerical results are provided and discussed to verify the theoretical results in Sections 4 and 5. Section 7 concludes the paper.

2. RELATED WORK

To deliver the cognitive information, the geographical area covered by the geo-location database is divided into small squares called pixels [8] or meshes [15] (where the mesh concept is used in this paper), which is the minimum granularity of environment information delivery. When the TVBD is within a mesh, it would query the database only once, and the TVBD will query the database again when it moves into a new mesh. Therefore, if the size of mesh is large, the cognitive information delivery is more efficient[‡], but less accurate. On the contrary, if the size of mesh is small, the cognitive information delivery is less efficient, but more accurate.

Several studies have been made on the accuracy of cognitive information delivery [4,6,8]. An accuracy standard ranged from 30 to 200 m is recommended in [6,8], which can be regarded as the length of a mesh's edge in this paper. However, most of these research works assume the same mesh size of 100 m × 100 m in a large geographical area, which needs further theoretical studies to validate what is the appropriate mesh size in terms of the accuracy and efficiency for the cognitive information delivery. Besides, the uniform mesh division is not an efficient solution.

For the cognitive radio networks with high mobility, such as cognitive radio vehicular networks, the delivery of spectrum information from the database to cognitive users, [16] and [17], apply the concept of interference alignment in a practical network setting, leading to dramatic reduction in message transmission times. With the scheme in [16] and [17], the number of queries and the probability of error are both reduced. In [18], Caleffi *et al.* model the database access problem as a Markov decision process and provide the closed-form expressions of the transition probabilities and maximize the expected TVWS communication opportunities through on-demand accesses to the database. To reduce the number of queries and reduce the load of geo-location database, Tran *et al.* [19] query the database with secondary user's preferred channels, but Tran *et al.* [19] do not reduce the number of database queries in the mobile environment.

3. PROBLEM STATEMENT

3.1. Cognitive Radio Database

We first describe the environment in this paper. In a specific area, there exist several TV networks[§]. The spectrum

[†]A smart utility network (SUN) is a ubiquitous network that facilitates efficient management of utilities such as electricity, water, natural gas, and sewage [12].

[‡]TVBDs need not query the database frequently

[§]In this paper, the TV network is called "network" for short.

bands of TV networks are not available for TVBDs within the coverage of the TV networks. However, the spectrum bands of TV networks are available outside the coverage of TV networks. The cognitive information that a TVBD receives contains the availability information of spectrums for this TVBD.

The entire region is divided into meshes, as illustrated in Figure 1. When a TVBD is located inside mesh #*i*, it can query the database for the cognitive information of mesh #*i* by providing its geographical information. A TVBD does not need to query the database again as long as it remains inside mesh #*i*, but needs to send query for a new cognitive information when moving out of mesh #*i* and entering a new mesh. Intuitively, the smaller the mesh, the smaller the error of cognitive information. However, the overhead of accessing the database and sending the query messages from TVBDs are higher.

In this paper, a mesh is denoted as “[*x*₁, *y*₁; *x*₂, *y*₂]”, where (*x*₁, *y*₁) and (*x*₂, *y*₂) are the coordinates of vertices on the diagonal of the (rectangle) mesh, with *x*₁ < *x*₂ and *y*₁ < *y*₂. Given a TVBD’s location coordinates as (*x*, *y*), the relation between the TVBD and the mesh is as follow.

$$TVBD_{is} \begin{cases} \text{inside the mesh} & \text{if } x_1 < x < x_2 \\ & \text{and } y_1 < y < y_2 \\ \text{outside the mesh} & \text{otherwise.} \end{cases} \quad (1)$$

Once the database receives the TVBD’s location coordinates, the database determines which mesh this TVBD is located in by (1). Then the database delivers the cognitive information of this mesh along with this mesh’s geographical information “[*x*₁, *y*₁; *x*₂, *y*₂]” to the TVBD. Accordingly, the TVBD can determine whether it is inside this mesh or not by (1). Once it detects that it is outside this mesh, it queries the database again for new cognitive information. Generally, the TVBD needs some localization technology such as GPS to determine its location.

3.2. Delivery of Cognitive Information

When a TVBD is located at the boundary area of a TV network, it is possible that partial area of the mesh where this TVBD locates is within a TV network, and the cognitive information of this mesh is not accurate. In this case, it is difficult to obtain accurate cognitive information from the database. Generally, the database transmits the cognitive

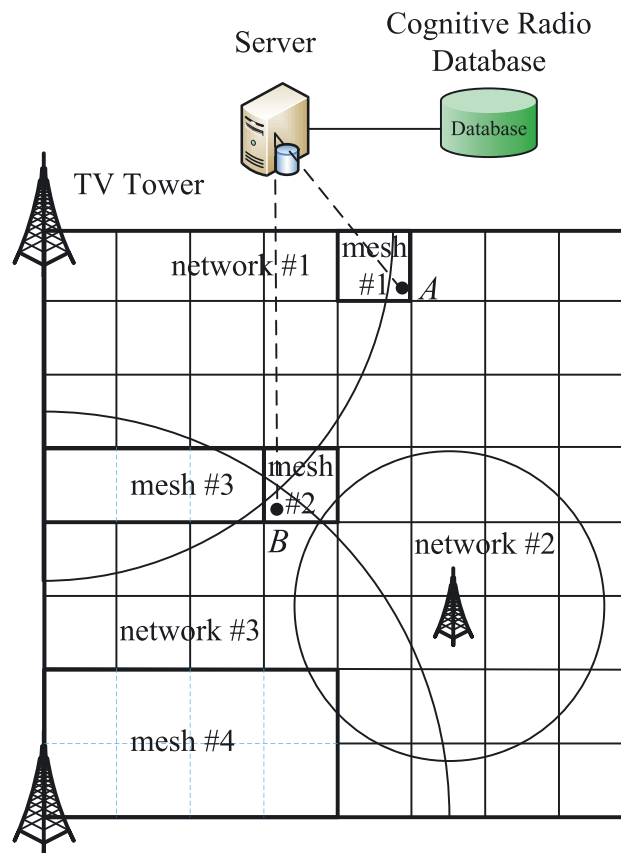


Figure 1. System model for cognitive information delivery.

information of the majority area of a mesh. This could lead to wrong channel availability information. For example, in Figure 1, the co-channel availability information of mesh #1 is

{Channels of network #1 are unavailable,
Channels of network #2 are available, (2)
Channels of network #3 are available}

When a TVBD appears at the point *A* of mesh #1, the channels of network #1 are available; however, the cognitive information in (2) declares that the channels of network #1 are unavailable, which is similar to the “false alarm” in spectrum sensing. When a TVBD is located at the point *B*, the channels of network #3 are unavailable; however, because the database sends the cognitive information of the majority area in mesh #2 to this TVBD, the co-channel availability information that this TVBD receives is

{Channels of network #1 are available,
Channels of network #2 are available, (3)
Channels of network #3 are available}

If TVBD access channels of network #3, it may interfere some TV receivers in the network #3. This situation is similar to the “missed detection” in spectrum sensing. Obviously, the smaller the mesh is, the smaller the probabilities of “missed detection” and “false alarm”. In this paper, we do not distinguish the “missed detection” and “false alarm”, but call them together as “radio parameter error (RPE)” for simplicity.

It is noted that the redundancy after regular mesh division exists, namely, there are adjacent meshes that contain the same cognitive information. Thus, we can fuse the adjacent meshes with the same cognitive information into one bigger mesh, for example, mesh #3 and mesh #4 in Figure 1 are the fusion results of some smaller meshes with the same cognitive information. The mesh fusion operation can reduce the frequency of database queries and improve the efficiency of cognitive information delivery without reducing the accuracy of cognitive information delivery, because it is more difficult for TVBDs to move out of a bigger mesh. There are some challenges associated with mesh fusion. In this paper, we will address the following two major issues:

- Providing the analysis on the relation between the size of mesh and the accuracy of cognitive information delivery, which is presented in Section 3.
- Designing efficient mesh fusion algorithm to reduce the redundancy of cognitive information, which is addressed in Section 4.

4. TRADEOFF BETWEEN THE EFFICIENCY AND ACCURACY OF COGNITIVE INFORMATION DELIVERY

In this section, we analyze the tradeoff between the efficiency and accuracy of cognitive information delivery. First, we address the representation of cognitive information.

4.1. Representation of cognitive information

The binary representation of network *k* at location (*x*, *y*) is

$$R(k, x, y) = \begin{cases} 1 & \text{if network } \#k \text{ is detected at } (x, y) \\ 0 & \text{otherwise} \end{cases} \quad (4)$$

which is similar to the representation in spectrum sensing, where “1” means the channels of network #*k* are busy and “0” means the channels of network #*k* are idle. The radio parameter at location (*x*, *y*) is characterized by the following summation of the binary representations for all networks [20].

$$I(x, y) = \sum_{k=1}^T R(k, x, y) \times 2^{k-1} \quad (5)$$

where *T* is the number of networks, (5) converts the binary number

“ $R(T, x, y), R(T-1, x, y) \dots R(1, x, y)$ ”

into a decimal number $I(x, y)$. The radio parameter of mesh #*i*, denoted as *P*, is the radio parameter of the majority area in mesh #*i* as follows.

$$P = \arg \max_j p_{ij} \quad (6)$$

where p_{ij} is the fraction of the area in mesh #*i* with radio parameter $I(x, y) = j$ due to (5) and $\sum_{j=1}^N p_{ij} = 1$. $N = 2^T$ is the number of radio parameters. Thus p_{ij} 's can be defined in a probability space. In (6), if p_{ij^*} is maximum, which means the fraction of the area in mesh #*i* with radio parameter j^* is maximum, then the radio parameter of mesh #*i* is j^* . In Figure 1, there are eight radio parameters, and the radio parameter of mesh 2 is 0 due to (5) and (6).

The RPE of mesh #*i* is defined as

$$p_{e,i} = 1 - \max_j p_{ij} \quad (7)$$

which is the remaining fraction except of the majority area in mesh #*i*. And the RPE of the entire region is defined as

$$p_e = \sum_{i=1}^M \alpha_i p_{e,i} \quad (8)$$

where M is the number of meshes and α_i is the area fraction of mesh $\#i$ compared with the area of the entire region.

We have $\sum_{i=1}^M \alpha_i = 1$. For regular (uniform) mesh division, $\alpha_i = \frac{1}{M}$.

4.2. Tradeoff between M and radio parameter error

In this section, we investigate the tradeoff between the number of meshes M and RPE.

Theorem 1. *The RPE of the entire region is $O\left(\frac{1}{\sqrt{M}}\right) \rightarrow 0$, where M is the number of meshes.*

Proof. The mesh that is distributed along the network boundary (shown as the solid curve in Figure 2) may contain impure radio environment, namely, the radio parameters (Equation (5)) of different spots in this mesh may be different. Denote the length of all these boundaries as ξ , the length of a mesh's edge as ε , and the length of the entire region's edge as L . Then, we have $M = \left(\frac{L}{\varepsilon}\right)^2$, and the number of meshes with impure radio environment is upper bounded by

$$K \leq \frac{2\xi\sqrt{2}\varepsilon}{\varepsilon^2} = \frac{2\sqrt{2}\xi}{\varepsilon} \tag{9}$$

which is obtained by considering the corresponding packing problem along the boundary, which is shown as the solid curve in Figure 2. Moving each point on this boundary in the two normal directions, a distance $\sqrt{2}\varepsilon$ gives the two dotted curves. The area between the two dotted curves is $2\xi\sqrt{2}\varepsilon$. All the meshes with impure radio environment are located between these two dotted curves; therefore, an upper bound of K is $2\xi\sqrt{2}\varepsilon$ divided by the area of a mesh.

Because $1 - p_{e,i} = \max_j p_{ij} \geq \frac{1}{N}$, we have

$$p_{e,i} \leq 1 - \frac{1}{N} \tag{10}$$

The RPE of the entire region is then upper bounded by

$$p_e \leq \frac{1}{M} K \left(1 - \frac{1}{N}\right) \leq \frac{1}{\sqrt{M}} \frac{2\sqrt{2}\xi L}{S} \left(1 - \frac{1}{N}\right) \tag{11}$$

$$E[\xi_i] = \int_0^{\frac{\pi}{4}} \left(\int_0^{\varepsilon \sin \theta} (x \tan \theta + x \cot \theta) f_X(x) dx + \int_{\varepsilon \sin \theta}^{\frac{\sqrt{2}\varepsilon \sin(\theta + \frac{\pi}{4})}{2}} \frac{\varepsilon}{\cos \theta} f_X(x) dx \right) f_{\Theta}(\theta) d\theta \tag{12}$$

$$E[p_{e,i}] = \int_0^{\frac{\pi}{4}} \left(\int_0^{\varepsilon \sin \theta} \frac{x^2 f_X(x)}{\varepsilon^2 \sin 2\theta} dx + \int_{\varepsilon \sin \theta}^{\frac{\sqrt{2}\varepsilon \sin(\theta + \frac{\pi}{4})}{2}} \left(\frac{x}{\varepsilon \cos \theta} - \frac{\tan \theta}{2} \right) f_X(x) dx \right) f_{\Theta}(\theta) d\theta \tag{13}$$

Theorems 1 shows the scaling law of the RPE as a function of M . The approximate result on the tradeoff between RPE and the number of meshes M is as follows.

Theorem 2. *The RPE as a function of M is*

$$p_e = \kappa \frac{1}{\sqrt{M}} \tag{14}$$

with

$$\kappa = \frac{\pi + \ln 64}{12\pi} \frac{\pi \xi}{-4\sqrt{2} \tanh^{-1}(1 - \sqrt{2})L} \tag{15}$$

where ξ is the length of the boundaries of all networks, L is the length of the entire region's edge, $\tanh^{-1}(z)$ is the inverse hyperbolic function defined as $\tanh^{-1}(z) = \frac{1}{2} \ln \frac{1+z}{1-z}$. κ is a constant, which is mainly determined by ξ and L .

Proof. Figure 3 illustrates the boundary of TV network in mesh $\#i$ with impure radio environment. This boundary can be approximated by a straight line when M is large. We ignore the situation when the boundaries of multiple networks cross a mesh, because the probability of this occurring is low when M is large. The parameters x and θ determine a line in Figure 3, where x is the distance between vertex A and the boundary, and θ is the minimum value of the angles between the mesh's edges and the horizontal line. Both x and θ are uniformly distributed random variables with probability density functions as follows.

$$f_{\Theta}(\theta) = \frac{4}{\pi}, 0 \leq \theta \leq \frac{\pi}{4} \tag{16}$$

and

$$f_X(x) = \frac{2}{\sqrt{2}\varepsilon \sin(\theta + \frac{\pi}{4})}, 0 \leq x \leq \frac{\sqrt{2}\varepsilon \sin(\theta + \frac{\pi}{4})}{2} \tag{17}$$

The length of the network boundary in the mesh is

$$\xi_i = \begin{cases} x \tan \theta + x \cot \theta & x \leq x_1 \\ \frac{\varepsilon}{\cos \theta} & x_1 < x < x_1 + \frac{x_2}{2} \end{cases} \tag{18}$$

where x_1 , x_2 , and x_3 are shown in Figure 3, with values

$$x_1 = x_3 = \varepsilon \sin \theta \tag{19}$$

$$x_2 = \left[\sqrt{2}\varepsilon \sin\left(\theta + \frac{\pi}{4}\right) - 2\varepsilon \sin \theta \right]^+ \tag{20}$$

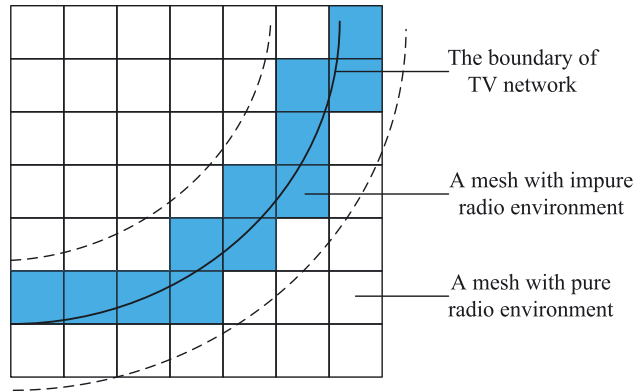


Figure 2. The boundary used to determine an upper bound on K .

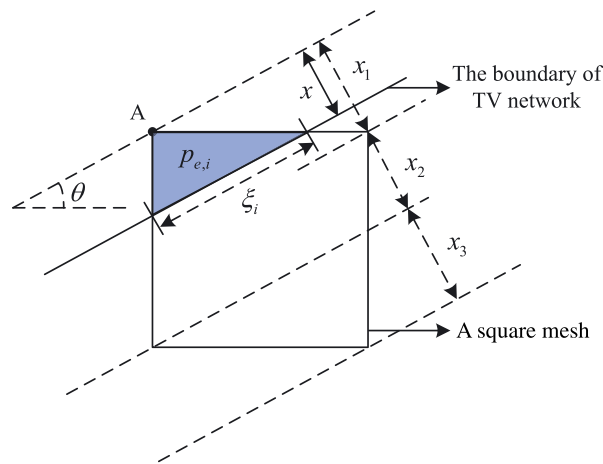


Figure 3. The boundary of TV network cuts a mesh whose edge length is ϵ .

with $[*]^+ = \max\{0, *\}$. The RPE of mesh # i is

$$p_{e,i} = \begin{cases} \frac{x^2}{\epsilon^2 \sin 2\theta} & x \leq x_1 \\ \frac{x}{\epsilon \cos \theta} - \frac{\tan \theta}{2} & x_1 < x < x_1 + \frac{x_2}{2} \end{cases} \quad (21)$$

The expectation values of ξ_i and $p_{e,i}$ are shown in (12) and (13) at the top of the next page, and the corresponding closed form expressions are

$$E[\xi_i] = -\frac{4\sqrt{2}\tanh^{-1}(1-\sqrt{2})\epsilon}{\pi} \cong 0.7935\epsilon \quad (22)$$

and

$$E[p_{e,i}] = \frac{\pi + \ln(64)}{12\pi} \cong 0.1937 \quad (23)$$

where $\tanh^{-1}(z)$ is the inverse hyperbolic function defined as $\tanh^{-1}(z) = \frac{1}{2} \ln \frac{1+z}{1-z}$. We determine the value of K , that is, the number of meshes with impure radio environment, using (22). Assume the first K meshes have an impure radio

environment, then we have

$$E[\xi_i] \stackrel{(a)}{=} \frac{1}{K} \sum_{i=1}^K \xi_i \stackrel{(b)}{=} \frac{1}{K} \xi \quad (24)$$

where (a) is due to the weak law of large numbers, and (b) is due to the fact that the meshes with impure radio environment cover all the boundaries of networks. The value of K can be estimated as

$$K = \frac{\xi}{E[\xi_i]} = \frac{\pi \xi}{-4\sqrt{2}\tanh^{-1}(1-\sqrt{2})\epsilon} \quad (25)$$

Assume the first K meshes have impure radio environment, then the RPE of the entire region is

$$p_e = \frac{1}{M} \sum_{i=1}^K p_{e,i} \stackrel{(c)}{=} \frac{K}{M} E[p_{e,i}] \quad (26)$$

where (c) is due to the law of large numbers. Substituting the value of K from (25) to the value of $E[p_{e,i}]$ from (23) into (26) gives

$$p_e = \frac{1}{\sqrt{M}} \frac{\pi + \ln 64}{12\pi} \frac{\pi \xi}{-4\sqrt{2}\tanh^{-1}(1 - \sqrt{2})L} \quad (27)$$

where ξ is the length of all the boundaries of networks, L is the length of the edges of the entire region, and N is the number of radio parameters. This is an approximate result. \square

Theorem 2 confirms Theorem 1. Further, we have $p_e = \Theta(\frac{1}{\sqrt{M}})$ according to Theorem 2. Note that RPE decreases with the increasing in M . Thus, Theorems 1 and 2 reveal the tradeoff between the accuracy and efficiency of cognitive information delivery.

5. MESH FUSION ALGORITHMS

The database for TV white spaces is generally constructed by estimating the signal strength using the (predicted) channel models. After the database is constructed, the mesh based cognitive information delivery scheme can be implemented. In order to know the radio environment around, a TVBD can send a query to the database along with its location, and the database will respond to the TVBD to indicate if certain frequency channels can be used and the geographical information of the mesh where the TVBD is located. If a TVBD moves outside the current mesh, it needs to send query again. In order to improve the efficiency of cognitive information delivery, the adjacent meshes with the same cognitive information can be fused into one bigger mesh in the database.

In this section, we first analyze the impact of the mesh fusion operation on RPE. We then propose two MFAs, regular mesh division and fractal-based mesh division, which are denoted as RMD-MFA and FbMD-MFA, respectively, to enable the database to efficiently fuse the mesh based on the radio environmental information. We also analyze the performance of the proposed algorithms.

In Section 3, the tradeoff between the number of meshes M (or the size of mesh) and RPE is investigated. The RPE decreases with the increase of M , while a large M will create extra overhead both to the database and TVBDs. Thus, we determine the number of meshes by upper bounding the RPE, namely, $p_e \leq \beta$. Substituting the value of p_e from (14) into the inequality $p_e \leq \beta$, we have achieved the required number of meshes to guarantee the RPE β as follows.

$$M \geq \left(\frac{(\pi + \ln 64)\xi}{12(-4\sqrt{2}\tanh^{-1}(1 - \sqrt{2}))L\beta} \right)^2 \triangleq M_1 \quad (28)$$

If the entire region is divided into $\lceil M_1 \rceil \times \lceil M_1 \rceil$ meshes, then the RPE of the entire region will not exceed β .

However, the redundancy of cognitive information with M_1 meshes exists, namely, there are adjacent meshes with the same cognitive information[¶]. Thus, we need to fuse the adjacent meshes with the same cognitive information into a bigger mesh to reduce the redundancy of cognitive information. In the following, we will analyze the impact of mesh fusion on the RPE and, then, design two mesh fusion algorithms.

5.1. Impact of mesh fusion on radio parameter error

Theorem 3. *If two meshes with the same radio parameters are fused, the RPE of the entire region remains unchanged.*

Proof. Assume two fusible meshes with the same radio parameters are mesh #1 and mesh #2. Before the mesh fusion operation, the RPE of the entire region is

$$p_e = \frac{s_1 p_{e,1} + s_2 p_{e,2} + \sum_{i=3}^M s_i p_{e,i}}{S} \quad (29)$$

where s_i is the area of mesh # i and S is the area of the entire region. The RPE of the fused mesh is

$$p_{e,\text{new}} = \frac{s_1 p_{e,1} + s_2 p_{e,2}}{s_1 + s_2} \quad (30)$$

Weighted by the area of the fused mesh, the RPE of the entire region after mesh fusion is

$$p_e^* = \frac{(s_1 + s_2)p_{e,\text{new}} + \sum_{i=3}^M s_i p_{e,i}}{S} = p_e \quad (31)$$

\square

Theorem 3 proves that the fusion of the meshes with the same radio parameters will not increase the RPE. Therefore, it is beneficial to support mesh fusion to reduce the number of meshes and, thus, the overhead to both the database and TVBDs without compromising the accuracy of cognitive information delivery. Thus, we will fuse the meshes with the same radio parameters.

5.2. Mesh division and fusion algorithms

The goal of mesh division and fusion algorithm is to cover the entire region with the minimum number of meshes, by fusing adjacent meshes with the same radio parameter into one bigger mesh. Two mesh division and fusion algorithms are designed in the following paragraph.

[¶]If two meshes have the same radio parameters, then the two meshes have the same cognitive information. Thus, in this paper, these two statements are equivalent.

In the first algorithm, the entire region is uniformly divided into regular meshes, denoted as RMD. We then fuse the meshes with the same radio parameters. We denote this algorithm as the RMD-MFA. The procedure of the second algorithm is to divide the unqualified mesh and retain the qualified mesh iteratively, where “qualified mesh” is defined as the mesh whose radio environment is almost pure. Because this algorithm adopts the iteration operation in fractal theory, it is denoted as FbMD. After FbMD, the adjacent meshes with the same radio parameters are fused. Therefore, the second algorithm is denoted as the FbMD-MFA.

5.2.1. Regular mesh division and mesh fusion algorithms.

As the entire region is uniformly divided into $[M_1] \times [M_1]$ regular meshes, an MFA is applied to fuse the meshes with the same radio parameters. If two meshes are fusible, they are not only geographically adjacent, but also have the same radio parameters, where the mesh's radio parameter is defined in (6). As illustrated in Figure 4, meshes $[x_1, y_1; x_2, y_2]$ and $[x_3, y_3; x_4, y_4]$ are fused into mesh $[\min_{i=1\dots 4} x_i, \min_{i=1\dots 4} y_i; \max_{i=1\dots 4} x_i, \max_{i=1\dots 4} y_i]$. If $mesh_i$ and $mesh_j$ are fusible, the relation is denoted as “ $mesh_i \longleftrightarrow mesh_j$ ”.

As in Figure 5, meshes are stored in a regular order after RMD. Thus, more efficient data structure can be designed to save the searching time in the MFA. In Figure 5, array map stores the right-adjacent and under-adjacent neighbors of a mesh, where 0 denotes an invalid mesh. Take i th column for an example, $map[1, i]$ is the index of mesh $\#i$, $map[2, i]$ is the index of right-adjacent mesh of mesh $\#i$, while $map[3, i]$ is the index of under-adjacent mesh of mesh $\#i$. As the adjacent mesh is stored in a regular order, the searching time can be reduced.

The parameters of the proposed algorithm are defined below: the entire region is divided into $N_m = [M_1] \times [M_1]$ meshes, where N_m is the total number of mesh. The radio parameter of each mesh is stored in an array $[f]_{N_m \times 1}$. MFA is described in Algorithm 1, whose key operation to update the mesh's neighbors after each mesh fusion.

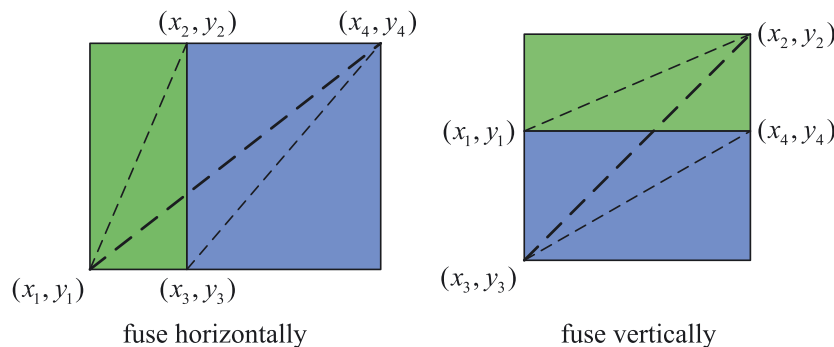


Figure 4. Mesh fusion operation

Algorithm 1 RMD-MFA

```

1: Divide the entire region into  $[M_1] \times [M_1]$  meshes.
2: Initialize  $map, label \leftarrow true$ ,
3: while  $label$  do
4:    $label \leftarrow false$ 
5:   for  $i = 1$  to  $N_m$  do
6:     if  $map[1, i] \neq 0$  then
7:        $L_r \leftarrow map[2, i]$ 
8:       if  $L_r \neq 0$  &  $mesh_i \longleftrightarrow mesh_{L_r}$  then
9:          $map[2, i] \leftarrow map[2, L_r], map[1, L_r] \leftarrow 0$ 
10:         $label \leftarrow true$ 
11:       end if
12:        $L_d \leftarrow map[3, i]$ 
13:       if  $L_d \neq 0$  &  $mesh_i \longleftrightarrow mesh_{L_d}$  then
14:          $map[3, i] \leftarrow map[3, L_d], map[1, L_d] \leftarrow 0$ 
15:         $label \leftarrow true$ 
16:       end if
17:     end if
18:   end for
19: end while

```

5.2.2. Fractal-based mesh division and mesh fusion algorithm.

Divide the entire region into $U \times U$ sufficient small pixels uniformly, where $U = 2^t$ and t is a positive integer. The pixel is the minimum spatial resolution during the processing. Take the coordinates of the center of each pixel as its geographical location. The radio parameter of each pixel with location (x, y) is $I(x, y)$ due to (5). The $I(x, y)$'s, namely, the radio parameters, are stored in a $U \times U$ matrix, denoted as Gra , which characterizes the cognitive information of the entire region.

Three key parameters are proposed for the FbMD, including *error limit*, *minimum edge of mesh*, and *stack of unqualified mesh*.

- *Error limit*: Denoted as σ_{\max} . According to (7), the RPE of one mesh is denoted in (32), where N_{I_k} is the number of pixels whose radio parameters are I_k by (5) in this mesh and N_B is the total number of pixels in

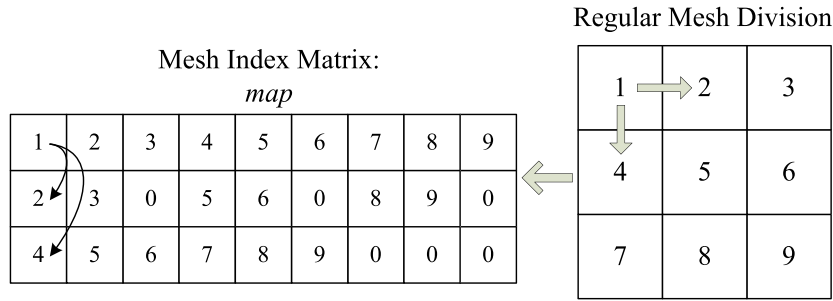


Figure 5. Data structure of mesh fusion algorithms in regular mesh division and mesh fusion algorithms

this mesh. A mesh is qualified if its RPE is smaller than σ_{max} , which means the radio environment of this mesh is almost pure.

$$RPE = 1 - \max_k \left\{ \frac{N_k}{N_B} \right\} \quad (32)$$

- *Minimum edge of mesh:* Denoted as e_{min} , which is the length of the shortest edge of a mesh. If a mesh's edge is shorter than e_{min} , it is also qualified, which means the mesh can not be further subdivided.
- *Stack of unqualified mesh:* Denoted as *stack*, which stores the unqualified meshes. In each iteration, the algorithm divides an unqualified mesh popped from the *stack*, then two smaller meshes will be generated. The qualified meshes among the two smaller meshes are stored in an array, denoted as *mesh*, while the unqualified meshes are stored in *stack* for the next iteration.

Fractal-based mesh division and mesh fusion algorithm is described in Algorithm 2, where each mesh is denoted by the coordinates of vertices on the diagonal, as well as the entire region, which is the first unqualified mesh. The division operation is defined as mesh $[x_1, y_1; x_2, y_2]$, which is divided into two smaller meshes: $[x_1, y_1; \frac{x_1+x_2}{2}, y_2]$ and $[\frac{x_1+x_2}{2}, y_1; x_2, y_2]$. The redundancy after FbMD still exists, namely, there are adjacent meshes with the same cognitive information. Thus, FbMD followed by MFA can further reduce the number of meshes. The MFA is described in the part II of Algorithm 2, which is different from the MFA in RMD-MFA, because the data structures of two algorithms are different. Note that, although we name "FbMD" as a mesh division algorithm, it can fuse the meshes compared with "RMD".

5.3. Analysis of regular mesh division mesh fusion algorithms

In MFA, mesh fusion results are illustrated in Figure 10, where the adjacent meshes with the same radio parameters are fused into one mesh. When iteratively fusing the meshes, we obtain the fusion results in Figure 10. The properties of MFA are summarized as follow.

Algorithm 2 FbMD-MFA

```

1: Part I. FbMD
2: stack  $\leftarrow$  the entire region, mesh  $\leftarrow \emptyset$ 
3: while stack is not empty do
4:   Pop mesh m from stack
5:   Divide m, get two smaller meshes  $m_1, m_2$ .
6:   for  $j = 1$  to 2 do
7:     if  $m_j$  is qualified then
8:       Append  $m_j$  to mesh
9:     else
10:      Push  $m_j$  in stack
11:    end if
12:  end for
13: end while
14: Part II. MFA
15: Get the number of meshes M; label  $\leftarrow true$ 
16: while label do
17:   label  $\leftarrow false$ ,  $i \leftarrow 1$ , get meshi
18:   while  $i \leq M$  do
19:      $j \leftarrow 1$ 
20:     while  $j \leq M$  do
21:       if  $mesh_j \longleftrightarrow mesh_i$  then
22:         Fuse  $mesh_i$  and  $mesh_j$ 
23:         Update array mesh,  $M = M - 1$ , label  $\leftarrow true$ 
24:       end if
25:        $j = j + 1$ 
26:     end while
27:      $i = i + 1$ 
28:   end while
29: end while

```

Theorem 4. In RMD-MFA, if the number of meshes before MFA is *M*, then the number of meshes after MFA is upper bounded by $(N^2 - N + 2)\sqrt{M} = \Theta(\sqrt{M})$. Thus, the number of meshes after MFA is $\Theta(\sqrt{M})$.

Proof. As illustrated in Figure 4, meshes can be fused horizontally and vertically. If we only fuse meshes horizontally, we obtain the upper bound of the number of meshes after MFA. According to Lemma 1, *N* convex-closed shapes (assume the shape of TV network coverage is convex) can divide the plane into $N^2 - N + 2$ parts at most. Thus, the types of radio parameters in a row is at most

$N^2 - N + 2$, and a row of \sqrt{M} meshes can be fused into $N^2 - N + 2$ meshes. We have \sqrt{M} rows of meshes; thus, the number of meshes after MFA is $(N^2 - N + 2)\sqrt{M} = \Theta(\sqrt{M})$. As we only consider horizontal fusion, this result is the upper bound. \square

Lemma 1. N convex-closed shapes (e.g., circle) can divide the entire plane into $N^2 - N + 2$ parts at most.

6. NUMERICAL RESULTS

In this section, we provide numerical studies to verify the proposed network design and to evaluate the performance of the mesh division and fusion algorithms.

6.1. Tradeoff between M and radio parameter error

The relation between the number of meshes M and the RPE is shown in Figures 6 and 7 for two scenarios with five and three TV networks, respectively, and the numerical results verify the theoretical analysis in Theorem 2. In Figures 6 and 7, RPE is a decreasing and convex function of M . Thus, the increase of M will reduce RPE and improve the accuracy of cognitive information delivery in the geo-location database. However, the increase of M will reduce the efficiency of cognitive information delivery. Thus, Figures 6 and 7 reveals the tradeoff between the accuracy and efficiency of the cognitive information delivery. The value of ξ in Figure 6 is larger than the corresponding value in Figure 7. Thus, to achieve the same

RPE, the number of meshes M in five TV networks scenario is bigger than that in three TV networks scenario. For example, to achieve the RPE = 0.04, the number of meshes with five TV networks is $M = 900$, which is much larger than that with three TV networks which needs $M = 289$. Because RPE is a convex function of M , thus when M is big, the RPE improvement is not noticeable. This indicates that too big M will not bring in higher benefit. The types of curves in Figures 6 and 7 can be applied to determine the number of meshes for a specific RPE requirement.

Based on the scenario of five TV networks in Figure 6, the different number of meshes M and corresponding RPE distributions are shown in Figure 8. The cognitive information of the entire region in Figure 6 is depicted in Figure 8 (a₁), (b₁) and (c₁) by 16×16 , 32×32 , and 64×64 meshes and the color of each mesh denotes different radio parameters. Moreover, (a₂), (b₂), and (c₂) are the RPE distributions of (a₁), (b₁), and (c₁), respectively. With the increase of mesh number, RPE is seen to decrease. Besides, RPE are always distributed around the boundaries of TV networks.

6.2. Mesh Fusion Algorithms

The result of mesh division and fusion algorithms are shown in Figures 9 and 10. The MFA in FbMD-MFA can reduce the number of meshes from 113 to 70. By fusing the adjacent meshes with the same radio parameters, the proposed FbMD-MFA can significantly reduce the number of meshes. Besides, the FbMD alone (without MFA) is also applicable, because the number of meshes in FbMD is much smaller compared with the uniform mesh division.

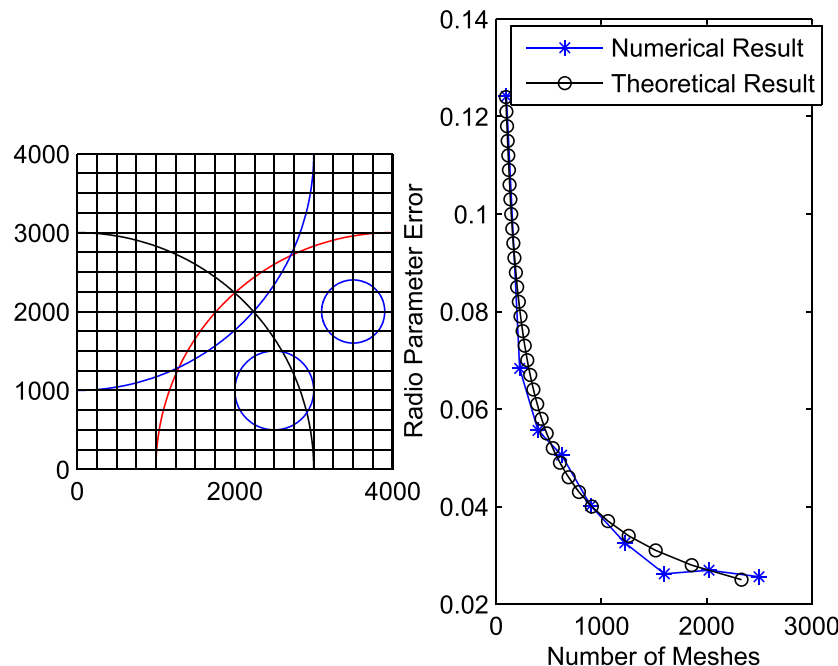


Figure 6. Five TV networks scenario (a) and the relationship between the number of meshes and the radio parameter error (b)

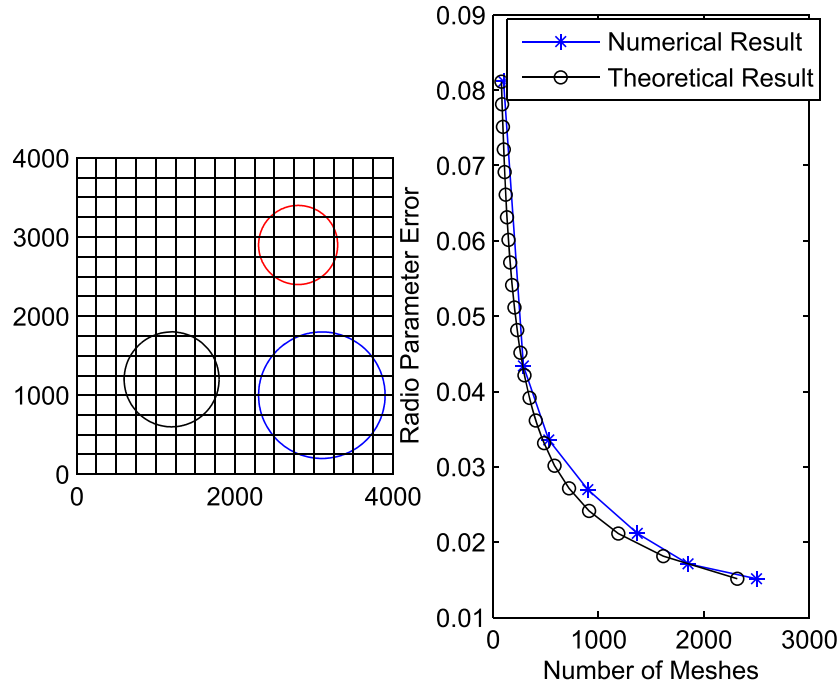


Figure 7. Three TV networks scenario (a) and the relationship between the number of meshes and the radio parameter error (b)

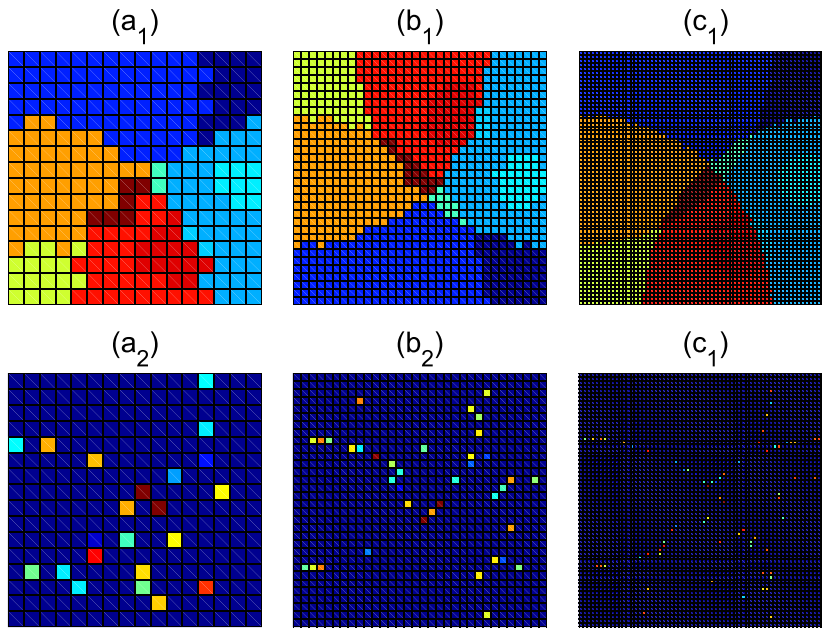


Figure 8. Radio parameter error distribution for TV networks: (a₁), (b₁) and (c₁) are the mesh division results with 16 × 16, 32 × 32, and 64 × 64 meshes, respectively; (a₂), (b₂), and (c₂) are the radio parameter error distributions of (a₁), (b₁), and (c₁), respectively.

The results of RMD-MFA with five and three TV networks are illustrated in Figure 10. The numbers of meshes in Figure 10(a) and (b) are much smaller than those in Figures 6(a) and 7(a), respectively. Thus, RMD-MFA can help greatly reduce the number of meshes and consequently the overhead for database access and TVBD

queries. In Figure 10, the number of meshes after fusion in a five network scenario is larger than that with three TV networks, because the radio environment of former is more complex than the later. Therefore, the distribution and number of networks also have impact on the performance of MFA. Figure 11 validates this observation. The

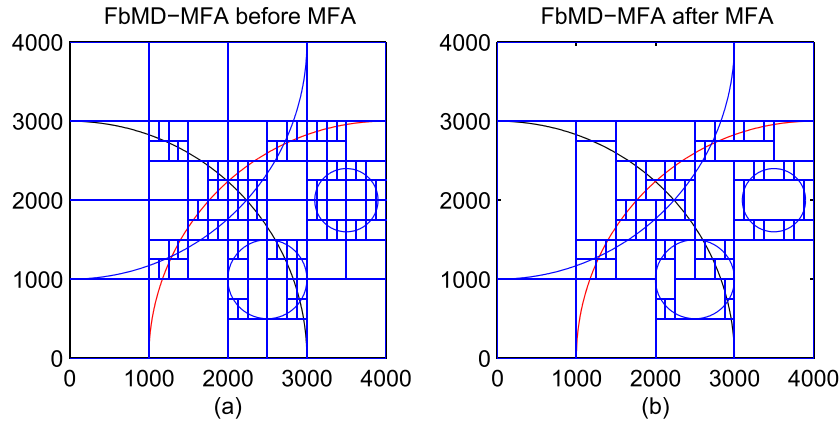


Figure 9. Results of fractal-based mesh division and mesh fusion algorithm.

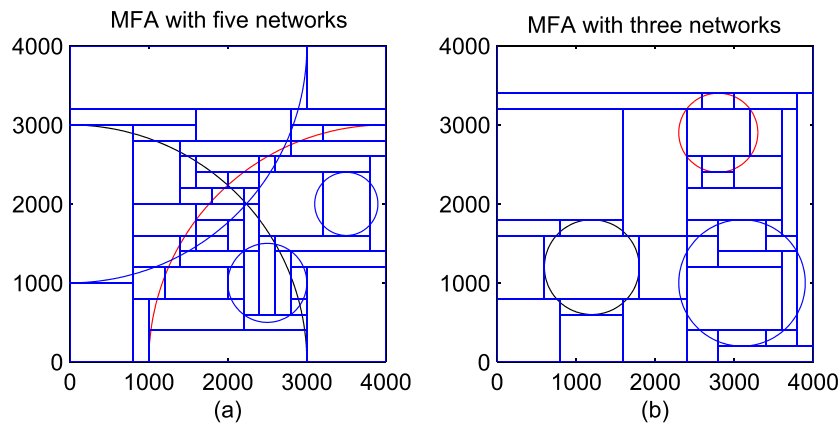


Figure 10. Results of regular mesh division and mesh fusion algorithm for five and three TV networks.

entire region is uniformly divided into different number of meshes, and we fuse the meshes with MFA. In Figure 11, the horizontal axis shows the number of meshes before MFA, and the vertical axis shows the number of meshes after MFA. MFA is shown to reduce the number of meshes, because the value of vertical axis is much smaller than that of the horizontal axis. Theorem 4 indicates that if the number of meshes before MFA is M , then the number of meshes after MFA is $Y = O(\sqrt{M})$, which is verified by Figure 11. The relation between Y and M for five TV networks by data fitting is

$$Y = 3.8076\sqrt{M} - 16.3808 \quad (33)$$

The relation between Y and M for three TV networks by data fitting is

$$Y = 2.7523\sqrt{M} - 8.3570 \quad (34)$$

In Figure 11, the data fitting results with five TV networks match very well with the corresponding numerical results, so are the data fitting results with three TV networks. Thus (33) and (34) are reasonable relation between

Y and M . Therefore, we have the relation $Y = O(\sqrt{M})$ and verify Theorem 4.

6.3. Number of database queries

In this section, the number of database queries is simulated and the key relations are verified. The TVBDs are uniformly distributed and moved following the random walk mobility model [21], where each node moves a distance v in a random direction in one movement. So v is defined as speed of movement. With these configurations, we simulate the mesh based cognitive information delivery scheme.

The TVBD obtains cognitive information via database. TVBD sends its location to the database, then the database feeds back to the TVBD, the cognitive information, and the geographical location information of the mesh where this TVBD locates. The TVBD can determine whether it is inside this mesh by (1). Once TVBD detects that it is outside this mesh, it re-queries the database for a new cognitive information. In this section, given a mesh division scheme and mobility model of TVBDs, we count the number of database queries.

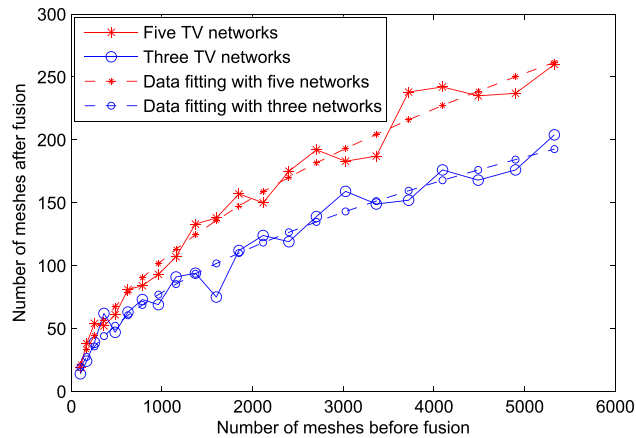


Figure 11. The number of meshes after mesh fusion algorithm (MFA) and before MFA in regular mesh division (RMD)-MFA.

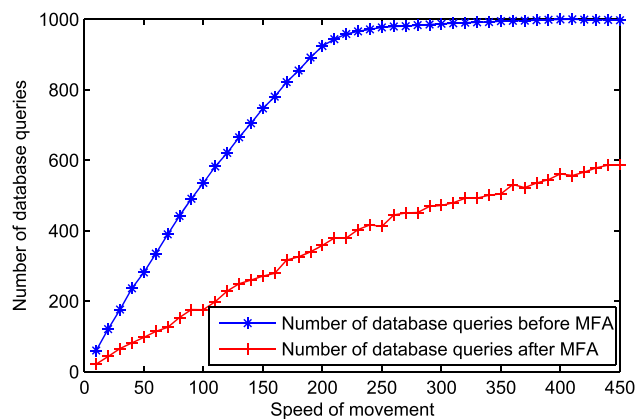


Figure 12. The number of database queries per TV band devices versus the speed for five TV networks (the TV networks are deployed as Figure 6 (a)).

In Figure 12, the relation between the number of database queries per TVBD and the speed of TVBD is provided. We deploy 100 TVBDs in the entire region, and each TVBD moves 1000 times. Note that the number of database queries increases with the speed. The number of meshes without MFA (Figure 6 (a)) is bigger than that with MFA (Figure 10 (a)). Thus, a TVBD is more likely to cross the boundary of a mesh without MFA, which will result in more frequent database queries. For the scheme without MFA, the length of a mesh's edge is small, thus when the speed of TVBD exceeds a threshold. A TVBD can always cross the boundary of the mesh in one movement, and the number of database queries per node is 1000, because each TVBD moves 1000 times in the simulation.

7. CONCLUSION

In this paper, to study the relation between the accuracy and efficiency of cognitive information delivery, we investigate the tradeoffs between the RPE and the number of meshes through analysis and obtain both the scaling function and approximate result. We also propose two mesh fusion

algorithms to improve the efficiency of the cognitive information delivery by reducing the number of meshes without sacrificing the accuracy. Numerical results have validated our theoretical results and demonstrated the efficiency of our mesh fusion algorithms. This paper provides a cognitive information delivery scheme, which can reduce the load of database and improve the efficiency of cognitive information delivery. The research of this paper provides a guideline for the implementation of database approach in cognitive radio networks. It is noted that this paper is still insufficient, the future works include the modeling of the cognitive information delivery using the mobility model of users and the implementation of this scheme in practice.

REFERENCES

1. White paper. *Cisco Visual Networking Index: Global Mobile Data Traffic Forecast Update, 2011–2016*. Cisco VNI Mobile: San Jose, USA, 2012.
2. McHenry MA. NSF Spectrum Occupancy Measurements Project Summary. *Technical Report*, Shared Spectrum Company, Vienna, USA, 2005.

3. Wang B, Liu KJR. Advances in cognitive radio networks: a survey. *IEEE Journal of Selected Topics in Signal Processing* 2011; **5**(1): 5–23.
4. Barrie M, Delaere S, Anker P, Ballon P. Aligning technology, business, and regulatory scenarios for cognitive radio. *Telecommunications Policy* 2012; **36**(7): 546–559.
5. ITU-R M.2225. Introduction to cognitive radio systems in the land mobile service, 2011.
6. FCC. Second Report and Order and Memorandum Opinion and Order: In the Matter of Unlicensed Operation in the TV Broadcast Bands, Doc. 08-260, 2008.
7. FCC. Second Memorandum Opinion and Order, Doc. 10-174, 2010.
8. ECC. Technical and operational requirements for the operation of white space devices under geo-location approach, ECC report 186, 2013.
9. Barrie M, Delaere S, Sukareviciene G, Gesquiere J, Moerman I. Geolocation database beyond TV white space? Matching applications with database requirements. In *Proceedings of the IEEE International Symposium on Dynamic Spectrum Access Networks (DySPAN)*, Bellevue, WA, 2012; 467–478.
10. Harrison K, Sahai A. Potential collapse of whitespaces and the prospect for a universal power rule. In *Proceedings of the IEEE International Symposium on Dynamic Spectrum Access Networks (DySPAN)*, Aachen, Germany, 2011; 316–327.
11. Ganapathy H, Madhavan M, Chetlur M, Kalyanaraman S. On exploiting degrees-of-freedom in whitespaces. In *Proceedings of IEEE INFOCOM*, Orlando, FL, USA, 2012; 1773–1781.
12. Sum CS, Harada H, Kojima F, Zhou L, Funada R. Smart utility networks in TV white space. *IEEE Communications Magazine* 2011; **49**(7): 132–139.
13. Wei Z, Feng Z. A geographically homogeneous mesh grouping scheme for broadcast cognitive pilot channel in heterogeneous wireless networks. In *Proceedings of the IEEE GLOBECOM Workshops*, Houston, TX, USA, 2011; 1008–1012.
14. Wei Z, Zhang Q, Feng Z, Li W, Gulliver TA. On the construction of radio environment maps for cognitive radio networks. In *Proceedings of the IEEE Wireless Communications and Networking Conference (WCNC)*, Shanghai, China, 2013; 4504–4509.
15. Zhang Q, Feng Z, Zhang G, Li Q, Zhang P. Efficient mesh division and differential information coding schemes in broadcast cognitive pilot channel. *Wireless Personal Communications* 2012; **63**(2): 363–392.
16. Al-Ali AK, Sun Y, Felice MD, Paavola J, Chowdhury KR. Accessing spectrum databases using interference alignment in vehicular cognitive radio networks. *IEEE Transactions on Vehicular Technology* 2015; **64**(1): 263–272.
17. Al-Ali A, Chowdhury K, Felice MD, Paavola J. Querying spectrum databases and improved sensing for vehicular cognitive radio networks. In *Proceedings of the IEEE International Conference on Communications (ICC)*, Sydney, NSW, Australia, 2014; 1379–1384.
18. Caleffi M, Cacciapuoti AS. Database access strategy for TV white space cognitive radio networks. In *Proceedings of the IEEE International Conference on Sensing, Communication, and Networking Workshops (SECON Workshops)*, Singapore, 2014; 34–38.
19. Tran HN, Alemseged YD, Chen S, Harada H. Reducing load of geo-location database by querying with secondary user's preferred channels. In *Proceedings of the IEEE 75th Vehicular Technology Conference (VTC Spring)*, Yokohama, Japan, 2012; 1–5.
20. Perez-Romero J, Salient O, Agusti R, Giupponi L. A novel on-demand cognitive pilot channel enabling dynamic spectrum allocation. In *Proceedings of the IEEE International Symposium on Dynamic Spectrum Access Networks (DySPAN)*, Dublin, 2007; 46–54.
21. Camp T, Boleng J, Davies V. A survey of mobility models for ad hoc network research. *Wireless Communications and Mobile Computing* 2002; **2**(5): 483–502.

AUTHORS' BIOGRAPHIES



Zhiyong Feng received her B.S., M.S., and Ph.D. degrees from Beijing University of Posts and Telecommunications (BUPT), China. Now, she is a professor at BUPT, and she is the Director of Key Laboratory of Universal Wireless Communications, Ministry of Education, P. R. China. She is a senior member of IEEE and active in standards development such as ITU-R WP5A/WP5D, IEEE 1900, ETSI and CCSA. Her main research interests include the wireless network virtualization in 5th generation mobile networks (5G), spectrum sensing and dynamic spectrum management in cognitive wireless networks, universal signal detection, and identification, network information theory, etc.



Zhiqing Wei received his B.S. and Ph.D. degrees from Beijing University of Posts and Telecommunications (BUPT) in 2010 and 2015, respectively. Now, he is a lecturer at BUPT. His research interests are capacity and delay analysis of cognitive radio networks and 5G wireless networks.



Qixun Zhang was born in 1983, China. He received B.S. and Ph.D. degrees in Telecommunication Engineering from Beijing University of Posts and Telecommunications (BUPT) in 2006 and 2011, respectively. Now, he is an Associate Professor at BUPT. His research interests include the resource management and performance analysis of heterogeneous wireless networks, wireless network virtualization in 5th generation mobile networks (5G), cognitive wireless networks, etc.



Wei Li received his Ph.D. degree in Electrical Engineering from the University of Victoria, Canada in 2004. He is currently a Senior Lecturer with Victoria University of Wellington and adjunct Assistant Professor with the University of Victoria, Canada. His research interests are in information theory and contemporary wireless systems, wireless sensor networks, and medical applications over wireless networks.



Xin Wang received the B.S. and M.S. degrees in telecommunications engineering and wireless communications engineering, respectively, from Beijing University of Posts and Telecommunications, Beijing, China, and the Ph.D. degree in electrical and computer engineering from Columbia University, New York, NY. She is currently an Associate Professor in

the Department of Electrical and Computer Engineering of the State University of New York at Stony Brook, Stony Brook, NY. Before joining Stony Brook, she was a Member of Technical Staff in the area of mobile and wireless networking at Bell Labs Research, Lucent Technologies, New Jersey, and an Assistant Professor in the Department of Computer Science and Engineering of the State University of New York at Buffalo, Buffalo, NY. Her research interests include algorithm and protocol design in wireless networks and communications, mobile and distributed computing, as well as networked sensing and detection. She has served in executive committee and technical committee of numerous conferences and funding review panels and is the referee for many technical journals. Dr. Wang achieved the NSF career award in 2005 and ONR challenge award in 2010.



Yi Qian is an Associate Professor in the Department of Electrical and Computer Engineering, University of Nebraska–Lincoln (UNL). Prior to joining UNL, he worked in the telecommunications industry, academia, and the government. Some of his previous professional positions include serving as a senior member of scientific staff and a technical advisor at Nortel Networks, a Senior Systems Engineer and a Technical Advisor at several startup companies, an Assistant Professor at University of Puerto Rico at Mayaguez, and a Senior Researcher at National Institute of Standards and Technology. His research interests include information assurance and network security, network design, network modeling, simulation and performance analysis for next generation wireless networks, wireless ad-hoc and sensor networks, vehicular networks, smart grid communication networks, broadband satellite networks, optical networks, high-speed networks, and the Internet. He has a successful track record to lead research teams and to publish research results in leading scientific journals and conferences. Several of his recent journal articles on wireless network design and wireless network security are among the most accessed papers in the IEEE Digital Library.